ELSEVIER

Ceramics International 29 (2003) 821–828

CERAMICS
INTERNATIONAL

www.elsevier.com/locate/ceramint

Sedimentation, rheology and particle-packing structure of aqueous Al_2O_3 suspensions

Wenjea J. Tseng[a,*], Chun Hsien Wu[b]

[a]Department of Materials Engineering, National Chung Hsing University, 250 Kuo Kuang Road, Taichung 402, Taiwan
[b]Institute of Materials Science and Manufacturing, Chinese Culture University, Yang Ming Shan, Taipei 11114, Taiwan

Received 22 November 2002; received in revised form 10 December 2002; accepted 5 January 2003

Abstract

Gravity settling, rheology and particle-packing structure of aqueous alumina suspensions have been investigated using submicrometer α-Al_2O_3 powders with an average particle size ~0.2 μm dispersed in pure water. The suspension pH varied from 2 to 11. The interface that separated the supernatant from the sediment appeared to settle linearly with time during the sedimentation experiment, followed then by a gradual reach toward a minimal sediment height; to which, the height was pH and solids loading dependent. The suspensions tended to form a continuous particulate network that defined the gravity settling as $\phi \geqslant 0.1$ at pH 11. This resulted in a flocculated suspension structure which barely settled even after 24 h without disturbance. The flocculated suspensions exhibited correspondingly a shear-thinning flow character over given shear-rate range ($\gamma = 1$–$1000\ s^{-1}$) examined, in contrast to an apparent transition of flow toward shear thickening from the shear thinning for the better-dispersed suspensions (pH = 2) at relatively high shear rates ($\gamma \geqslant 100\ s^{-1}$). This finding suggested a breakdown of the particulate network into smaller flow units for the flocculated suspensions as shear rate was increased. Films made from the flocculated suspensions showed apparent cracking after drying. Microstructural examinations revealed that a pronounced grain growth occurred in the films made from the pH 2 suspensions after isothermal sintering.

Keywords: A. Grain growth; D. Al_2O_3; Sedimentation; Rheology; Aggregation

1. Introduction

Dispersion of particulate materials in liquid medium and the associated rheological property of the suspensions are of fundamental importance to slurry-forming fabrication processes of ceramics [1–7]. The processes generally rely on the development of an electrostatic and/or a steric barrier layer around particle surfaces in liquid, so that the interparticle forces between neighboring particles can be optimized to a satisfactory level [1]. This enables the forming processes to be carried out in a reduced viscosity for facilitating the suspension flow [4–7]. The consolidated article thus formed demands a uniform particle-packing structure for avoiding generations of inhomogeneities that may become disproportionately pronounced in the following firing processes, such as during thermal debinding and sintering [8].

Using water as a liquid vehicle for powder dispersion and slurry forming is advantageous from both a cost and environmental perspective. Practices for attaining a stable colloid often involve a proper control of colloidal pH in a way that the pH value is sufficiently away from the isoelectrical point (IEP) of the powder in a given liquid, with an aim of forming sufficient repulsion between particle surfaces [4,9]. Dispersion is also attainable through a minor addition of polyelectrolyte surfactant that is able to anchor one end of the surfactant molecule onto the particle surface while presenting the other end stretching toward the liquid for providing the steric (and/or electrosteric) repulsion required for slurry stabilization [9–11]. While the dispersion/stabilization of aqueous powder suspensions has been studied extensively in the literature [1,2,4–9], little attention has been devoted to examining the correlation between the particle dispersion to the "macroscopic" flow property [1,5,9] and the "resultant" sintered microstructure of the formed compacts. The present study attempted to provide such a

---

* Corresponding author. Tel.: +886-4-2287-0720.
E-mail address: wenjea@dragon.nchu.edu.tw (W.J. Tseng).

0272-8842/03/$30.00 © 2003 Elsevier Ltd and Techna S.r.l. All rights reserved.
doi:10.1016/S0272-8842(03)00023-3

link by examining the sedimentation behavior of a model alumina suspension system dispersed in pure water at various pH values and solids concentrations, and to compare the gravity-settling behavior to the suspension rheology over a wide range of shear rate (1–1000 s^{-1}) typically encountered in most of the slurry-forming processes of ceramics [12]. Some Al_2O_3 suspensions were fabricated into thick films via an electrophoretic deposition (EPD) method, and their sintered microstructures were also examined.

2. Experimental procedure

Alumina powder (AKP-50, Sumitomo, Japan) with an average particle size ~0.2 μm was used as the starting material. The powder was about spherical in shape [13] from the observation of scanning electron microscopy (SEM, JSM-6335F, JEOL, Japan) and presented a major phase of α-Al_2O_3 from X-ray diffractometry (MAC Science, M18X-1180, Japan) using CuK_α radiation.

The powder was first dried in oven at 110 °C for 24 h to remove any moisture adsorbed on the powder surface before being mixed with double-distilled water in volumetric solids ratio (ϕ) of 0.01–0.15. The pH of the mixtures was adjusted by addition of reagent-grade HCl or NH_4OH (Ging-Ming Chemicals, Taiwan) to pre-determined levels of pHs 2 and 11 in a way that the addition of chemicals did not influence the overall solids concentration much ($\Delta\phi < 0.0005$ typically). The powder mixtures were then ball-mixed using 10 mm high-purity alumina balls in polyethylene bottles for a period of 24 h before the pH being re-examined and adjusted to the pre-set values if necessary. The slurries were then slightly mixed again and then transferred to graduated cylinders (diameter ~1.5 cm, height ~15 cm) to a height of 10 cm. The cylinders were capped to minimize water evaporation and left undisturbed for the gravity sedimentation. The top interface that separates the supernatant from the sediment was measured over a period of time up to 24 h after the suspensions were poured into the cylinders. The interface was easily distinguishable for the flocculated suspension system; of which, the particles settled toward the bottom of the cylinder rather quickly, leaving behind a clear supernatant. Nonetheless, the interface might become difficult to discern in a system with a relatively "good" dispersion. This hence might lead to some experimental errors in the better-dispersed suspensions, considered acceptable from a qualitative viewpoint for suspension stability [13–15].

The rheological properties of the aqueous suspensions were determined using a strain-controlled concentric viscometer (VT550, Gebruder HAAKE Gmbh, Germany) equipped with a sensor system (MV-DIN 53019, HAAKE, Germany) of cone-cup geometry at constant temperature (25 °C). The measurement was performed with a steady increment of shear rate (γ) over a shear-rate range 1–1000 s^{-1}. Experimental details about the rheological measurement have been reported elsewhere [13,16,17].

For the EPD forming of the colloidal suspensions, the suspensions in solids concentrations of 0.05, 0.1 and 0.15 at pH 2 were placed in glass cells. The EPD was conducted at a constant voltage of 30 V using graphite as an anode and copper as a cathode substrate placed 2 cm away from the anode in a face-to-face separation [17]. The deposited Al_2O_3 on the cathode surface was in a form of porous films typically 500 μm in thickness. The films were then peeled off from the substrates, followed by oven-drying at 60 °C for 48 h before being sintered at 1050 °C with a constant heating rate of 10 °C min^{-1} and an hour isothermal holding in air atmosphere. Sintered microstructure of the EPD membrane films was examined by SEM.

3. Results and discussion

3.1. Sedimentation behavior of the Al_2O_3 suspensions

The gravity-settling behavior of the aqueous Al_2O_3 suspensions at different solids concentrations (ϕ) is shown in Fig. 1a and b for the suspensions at pH 2 and 11, respectively. The suspensions appeared to settle linearly with time initially, followed then by a gradual reach toward a minimal sediment height as time lengthens (up to 24 h), except for the suspensions of $\phi \geqslant 0.1$ at pH 11. The suspension height-settling time dependence remained linear up to ~10^4 s for the pH 2 case; whilst, the linearity was about an order shorter in terms of the time frame (~2×10^3 s for $\phi \leqslant 0.03$) as the suspension pH changed to 11. This indicates that the attractive van der Waals force prevailed over the interparticle potential at the pH 11 case. The interparticle attraction would compete with the gravitational force during the particle sedimentation [14,15] and appeared to prevail over the gravitational force at the initial stage of the settling, so that the particles in suspensions tended to form aggregates at pH 11 and the aggregated clusters of undetermined size led to the increased settling velocity observed. Fig. 1 shows a reduced particle-packing density for the formed sediment of varying solids fractions, featured apparently with a comparatively higher sediment height in the flocculated case (pH 11) than that of the better dispersed state (pH 2) after deposition. This finding was in parallel with the particle/cluster aggregation and settling velocity of the suspensions observed, since the settling particles would rearrange themselves toward a denser packing configuration in the case that the interparticle attraction is diminished to a significant degree with an improved dispersion.

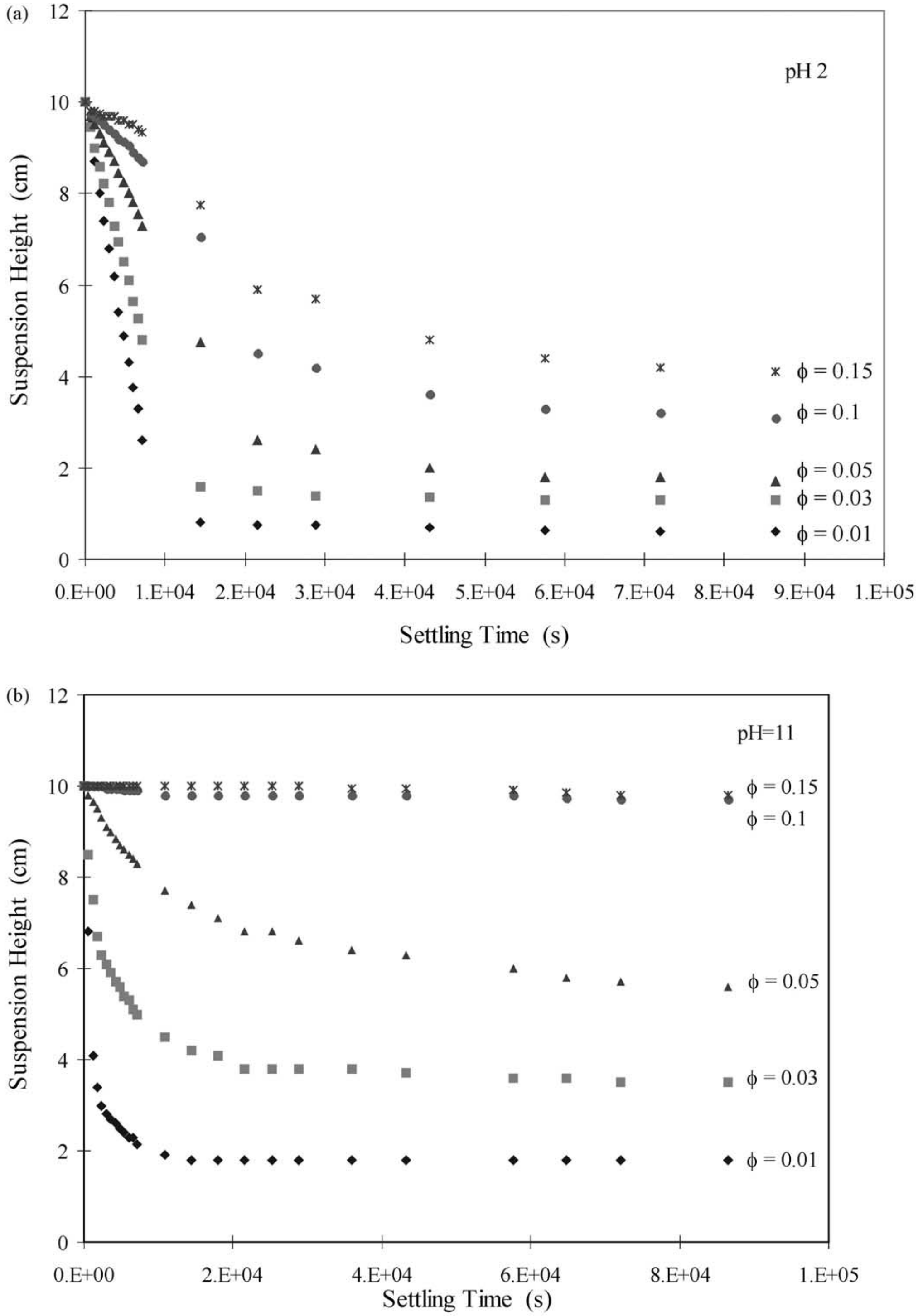

Fig. 1. Sedimentation behavior of aqueous Al_2O_3 suspensions of various solids fractions at (a) pH 2, and (b) pH 11. The suspensions were left undisturbed in graduated cylinders over a period of 24 h.

The IEP of the α-Al_2O_3 powder in water has been reported to be about 9–9.5 [12]. The stability found in our aqueous Al_2O_3 suspensions was hence presumably attributed to the difference (in magnitude) of the electrostatic forces taking place at the interparticle distance by the double-layer repulsions that occurred at the pH examined [4,9]. This further suggested a reduced double-layer repulsion was resulted at the pH 11 case than that of the pH 2 case in the model suspensions.

The ‘‘initial’’ settling velocity of the particles (even though vaguely defined here at present) in the liquid medium is attempted to correlate with the structure of suspensions. One would suspect that spatial re-structuring in an undetermined form would probably occur within the particle clusters during gravity settling; of which, fracture might occur within the particulate clusters thus facilitating water flow in an upward direction [15]. The settling velocity (U) of the clusters is related to the solids fraction by the Richardson-Zaki equation [14]:

$$U = U_o \cdot (1 - \phi)^m \tag{1}$$

where U_o is the settling velocity of an isolated sphere in liquid, ϕ is the volumetric solids fraction, and the exponent m is related to the sensitivity of the settling velocity to the solids concentration in suspension. The U_o is related to the Stokes' law by

$$U_o = 2\Delta\rho a^2 g/9\eta \tag{2}$$

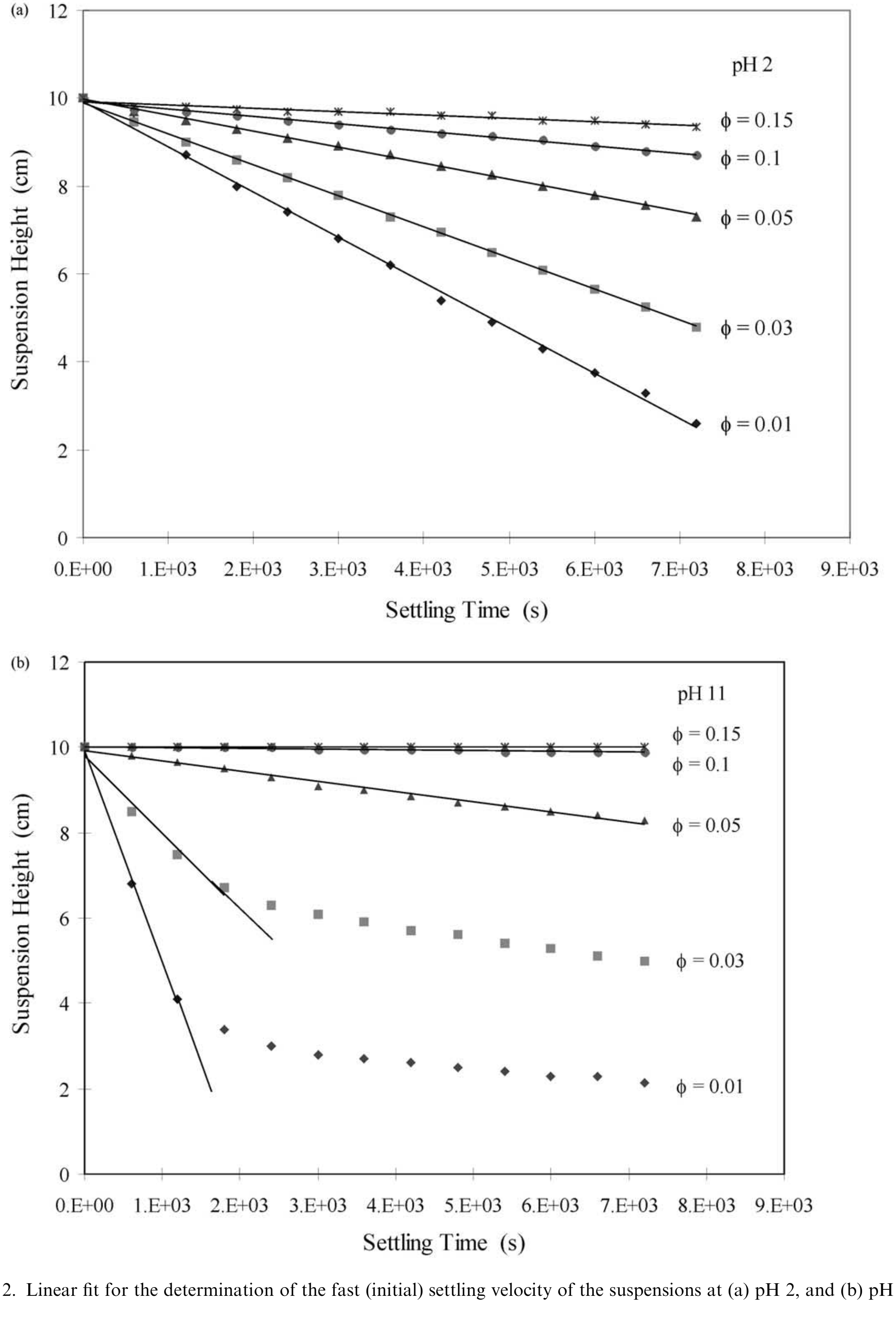

Fig. 2. Linear fit for the determination of the fast (initial) settling velocity of the suspensions at (a) pH 2, and (b) pH 11.

where $\Delta\rho$ is the difference between the density of particle and that of the suspending liquid, a is the particle radius, g is the settling acceleration due to gravity, and η is the viscosity of the carrier liquid.

Fig. 2 shows the linear fit for the determination of the fast (''initial'') settling velocity (U) of the suspensions. The interface that separates the supernatant from the sediment appeared to behave linearly with the settling time over the ''initial'' time frame chosen. Even the time frame chosen appeared a bit arbitrarily, a typical correlation factor (R^2) greater than 0.99 was resulted for the fitted lines over the time period (up to $\sim 7\times 10^3$ s) and solids-concentration range ($\phi = 0.01$–0.15) at suspensions of pH 2. For the pH 11 suspensions, however, the linearity was only ''valid'' in a substantially short time period (especially for suspensions with $\phi \leqslant 0.03$). Fig. 3 shows the relationship between the settling velocity and the solids fraction expressed in $(1-\phi)$ form at different pH values. The lines indicated in the figure are the power-law fit of the experimentally attained data. Both the suspensions at pHs 2 and 11 appeared to follow the Richardson-Zaki equation reasonably well. The exponent values ($m = 17$ at pH 2 and $m = 58.7$ at pH 11) were yet substantially larger than that of the colloidal SiO_2 system ($m = 4.63$) reported by Guo and Lewis [14]. The comparatively large exponents found in the suspensions reveal a strong dependence of the settling velocity (U) to the solids fraction ϕ in our model system, particularly for the pH 11 suspensions. This non-linear dependence seemed to become much more pronounced as the solids concentration approaching toward a more dilute situation (i.e., as $(1-\phi)\rightarrow 1$), and was apparently pH specific. The flocculated system yielded a larger exponential dependence, indicating the Richardson-Zaki form is structure-sensitive.

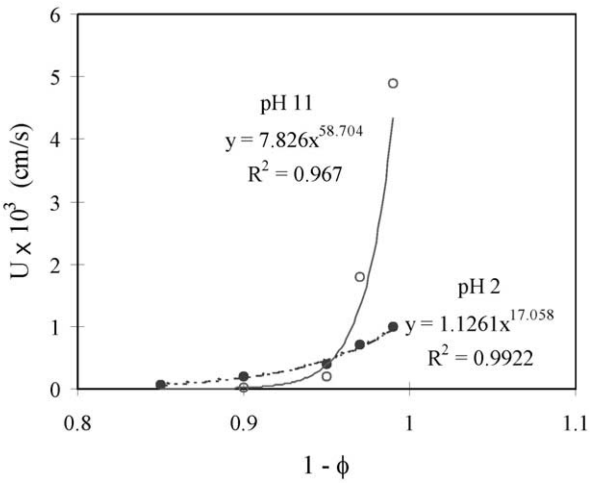

Fig. 3. The Richardson-Zaki fit of the settling velocity to the solids fraction for the Al_2O_3 suspensions at the initial stage of the sedimentation experiment.

3.2. Rheological behavior of the Al_2O_3 suspensions

The flow behavior of the suspensions is shown in Fig. 4 over a shear-rate range from 1 to 1000 s^{-1}. All the suspensions exhibited a shear-thinning flow character at low shear-rates regime; followed then by a shear-thickening flow as the shear rate exceeded a certain critical rate. The shear-thinning flow indicated the particle aggregations existing in the slurry were broken down into smaller flow units as shear rate increased. As shear rate further increased, suspension structure would tend to become more uniformly packed [16], leading to the reduced shear viscosity. The ordered structure appeared to be ''suddenly'' disrupted as γ approached γ_{onset}. This indicated a more random-typed structure was resulted in the suspensions so that a larger packing volume was required for the suspension flow and hence resulted in an increased viscosity. The critical level (γ_{onset}) for the flow transition appeared to be solids loading and suspension pH dependent, as indicated in Table 1. At lower solids concentrations ($\phi = 0.03$ and 0.05), the scattering in suspension viscosity was more pronounced and this was presumably due to the viscosity values approached toward the lower bound of the detection limit of the viscometer sensor employed for the measurement. Nonetheless, the shear-thickening flow was still apparent. Additionally, the critical shear rate (γ_{onset}) appeared to increase toward higher shear-rate levels as ϕ was increased for both pH cases (Fig. 4). This is believed partly due to the stronger interparticle interactions involved in the more concentrated suspensions, which tend to ''preserve'' the attractive particulate structure to higher shear rates.

The rheological behavior compared favorably with the gravity settling of the suspensions shown in Fig. 1, and further substantiated the previous assumptions in the formation of a continuous particulate network in the flocculate suspensions. By contrast, the sedimentation experiment failed to provide details in the structural change in the network as flow proceeded, especially for suspensions of $\phi = 0.1$ and 0.15 at pH 11. In this regard, the viscosity determination provides a

Table 1
The critical shear rate (γ_{onset}) for the onset of the suspension shear-thickening to occur

Suspension	γ_{onset} (s^{-1}) at various solids fractions			
	$\phi = 0.03$	$\phi = 0.05$	$\phi = 0.10$	$\phi = 0.15$
pH 2	80*	80*	100	300
pH 11	100*	300	800	N.A.

The critical shear rate (γ_{onset}) with asterisk mark is for reference purposes since the viscosity measured may contain substantial scatterings due presumably to the detection limit of the sensor employed.

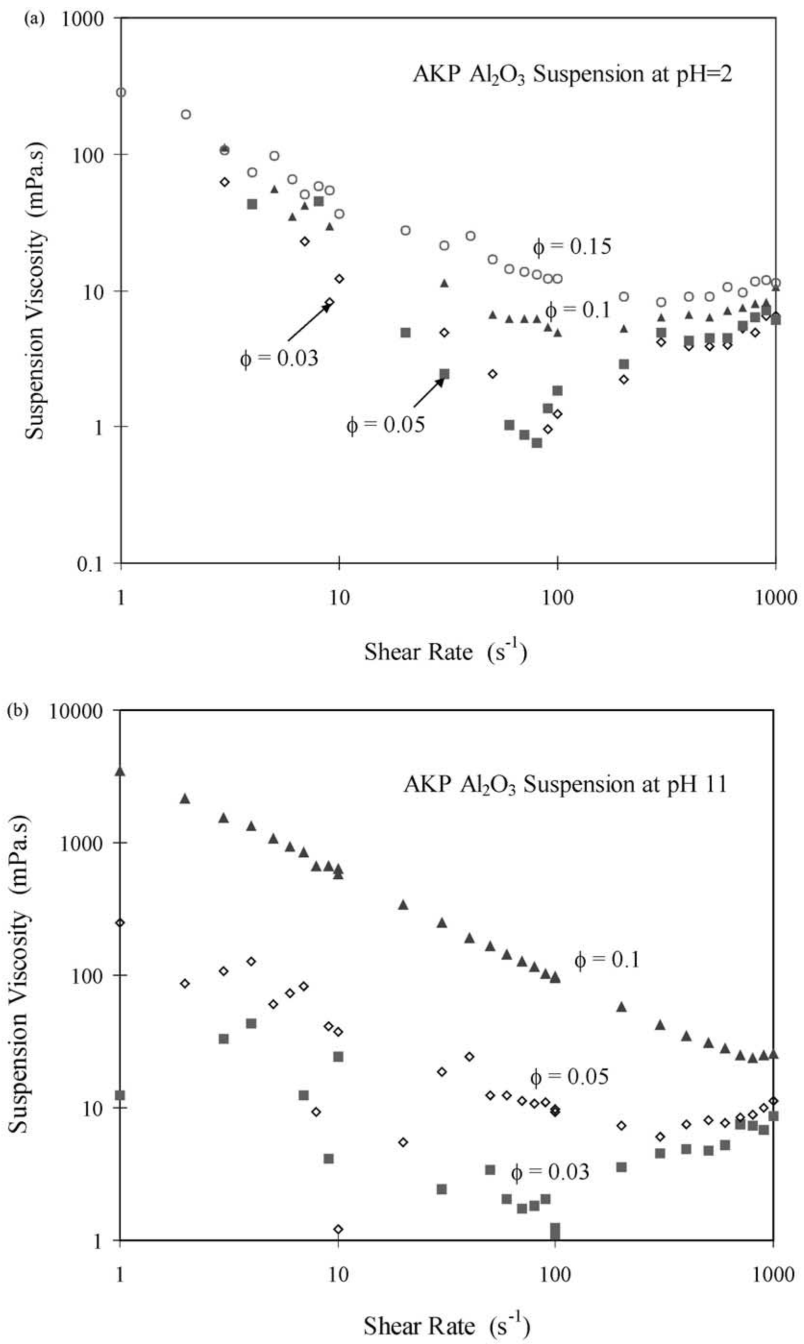

Fig. 4. Viscosity- shear rate dependence of the Al_2O_3 suspensions at (a) pH 2, and (b) pH 11.

better insight allowing a clear distinction between the two strongly flocculated suspensions (ϕ of 0.1 and 0.15 at pH 11) than that of the "qualitative" sedimentation method.

The particles in the suspensions needed to overcome a yield stress before they can roll over neighboring ones for the flow to occur. The yield stress of the suspension (τ_y) can be determined by the Casson's equation [18] given as

$$\tau^{1/2} = \tau_y^{1/2} + \eta\gamma^{1/2} \tag{3}$$

where τ is the apparent shear stress of the suspension, η the suspension viscosity, and γ the apparent shear rate. The yield stress (τ_y) is determined from a linear extrapolation of the $\tau_y^{1/2}$–$\gamma^{1/2}$ dependence to $\gamma^{1/2}=0$. Fig. 5 shows the suspension τ_y increased with ϕ; in particular, the τ_y–ϕ dependence becomes highly nonlinear for the pH 11 suspensions. This disproportionally increased τ_y value was considered a clear indication of the strongly flocculated (unstable) nature of the suspensions [10], which also substantiated in part to the existence of the particulate network discussed above.

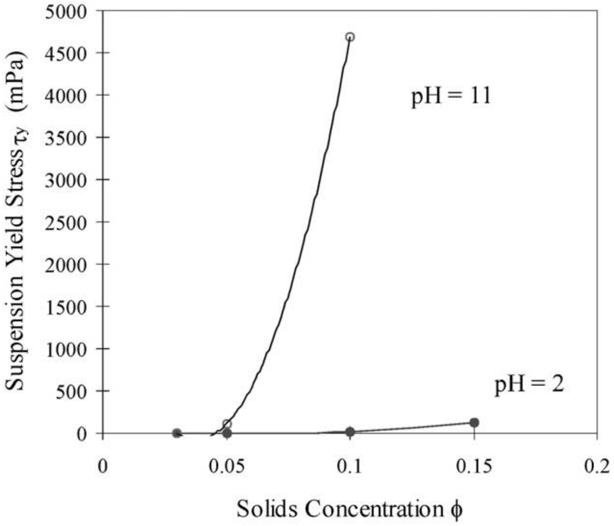

Fig. 5. Dependence of the suspension yield stress (τ_y) to the solids concentration of the Al_2O_3 suspensions at pHs 2 and 11.

3.3. Particle-packing structure of the EPD films

Alumina thin sheets were fabricated using the suspensions of the better dispersed, i.e., the pH 2, suspensions by the EPD method. We have also tried using the pH 11 suspensions for the EPD. All the dried films from the pH 11 suspensions formed apparent cracks after ambient-atmosphere drying. This suggested that the deposited films presented a non-uniform particle packing presumably due to the flocculated nature of the suspensions (at pH 11) which led to the cracking observed.

Fig. 6 shows the fractured microstructure of the cross-sectional view of the EPD membranes (from pH 2 suspensions) sintered at 1050 °C for 1 h. Typical thickness of the films was about 500 μm, and the cross-sectional microstructure remained the same throughout the thickness of the samples. A pronounced grain growth was seen as $\phi \geqslant 0.10$ (Fig. 6b and c). This finding together with the

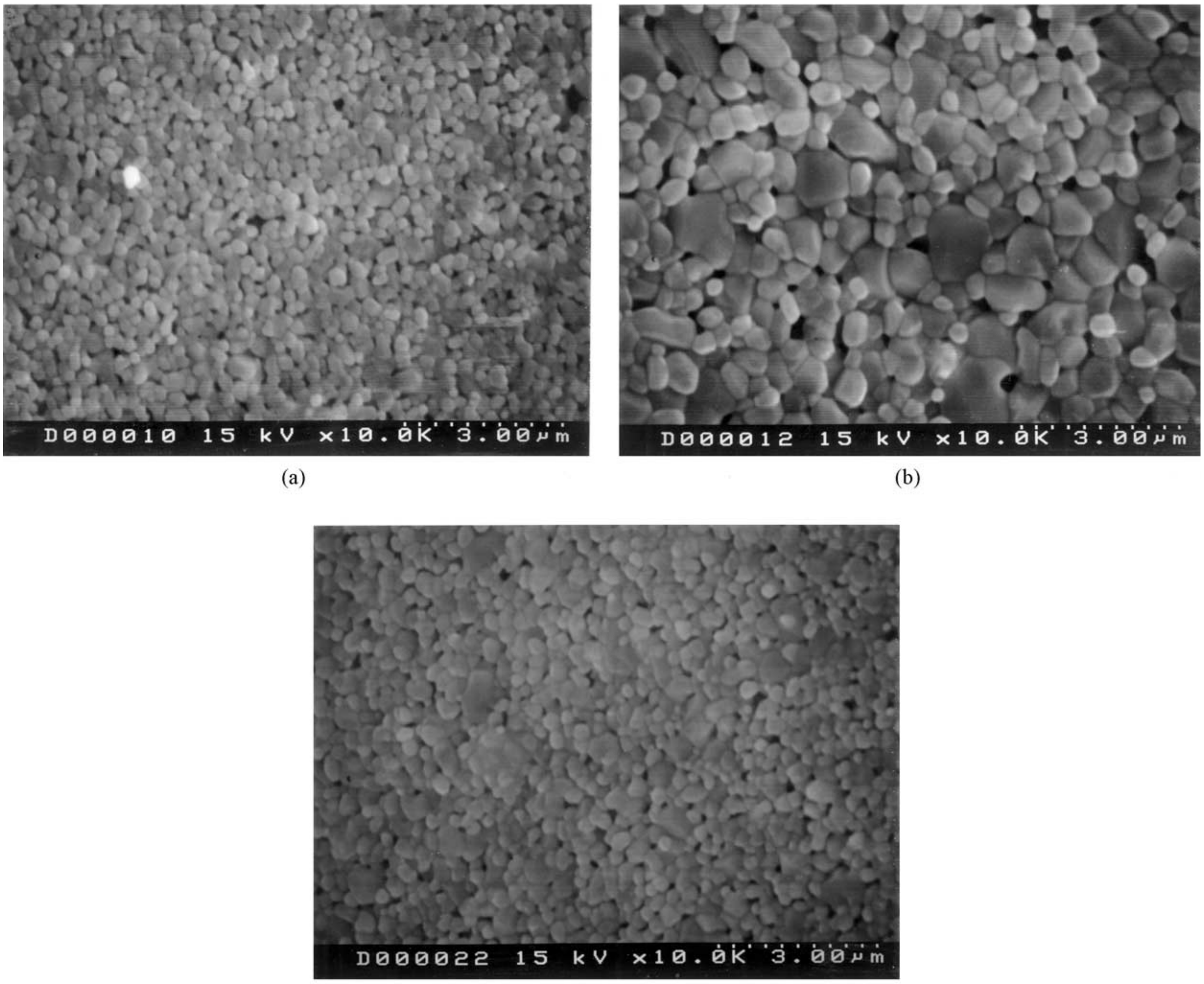

(a) (b)

(c)

Fig. 6. Microstructure of EPD-deposited Al_2O_3 membranes from the suspensions of solids fraction (a) 0.05, (b) 0.1, and (c) 0.15. The films have been sintered at 1050 °C with 1 h isothermal holding.

apparent disappearance of the interconnected pore at the particle/grain contacts suggested that the film density increased as ϕ exceeded 0.05, so that a faster sintering rate was resulted and also as $\phi \geqslant 0.10$ which led to the grain growth observed. Increasing the solids loading of the suspensions might hence facilitate the electrophoretically deposited particle-packing structure toward a more densely packed configuration that in turn promoted the powder densification at elevated temperatures.

4. Conclusions

The cluster settling and rheological behavior of submicrometer Al_2O_3 suspensions have been examined at different solution pHs (pHs of 2 and 11) and solids concentrations. The suspension presents a better dispersion stability at pH 2, resulting in a turbid suspension slowly forming a densely packed configuration as time lengthens. Rheology of the pH 2 suspensions shows in parallel a shear-thinning flow followed then by a shear-thickening flow character at high shear rates. Contrarily, the particles in pH 11 tend to aggregate at the beginning of the sedimentation. The gravitation force eventually prevails over the particle interaction, accelerating the settling of the aggregate clusters at the initial stage of the settling. As the solids concentration was raised above 0.1 (pH 11), the particles appear to form a continuous gelled network that defies the gravity settling and results in a porous packing structure with a reduced sediment density. The suspension flow changes toward predominately a shear-thinning flow character over the shear-rate range examined, indicative of the flocculated nature of the suspensions. The better-dispersed suspension (pH 2) facilitates the EPD forming of porous alumina films, resulting in un-cracked green sheets after drying. Increasing the solids concentration of the suspension (pH 2) appears to promote the powder densification during sintering.

Acknowledgements

The authors gratefully acknowledge financial support from the National Science Council (Taiwan) under contract NSC 89-2216-E-034-015. We would also like to thank Mr. Kuo-Hsing Teng for his assistance in microstructural observations.

References

[1] J.A. Yanez, T. Shikata, F.F. Lange, D.S. Pearson, Shear modulus and yield stress measurements of attractive alumina particle networks in aqueous slurries, J. Am. Ceram. Soc. 79 (11) (1996) 2917–2924.

[2] S. Desset, O. Spalla, P. Lixon, B. Cabane, From powders to dispersions in water: effect of adsorbed molecules on the redispersion of alumina particles, Langmuir 17 (2001) 6408–6418.

[3] P. Somasundaran, X. Yu, Dispersions: progress and prospects, Powder Technol. 88 (1996) 305–307.

[4] R.G. Horn, Surface forces and their action in ceramic materials, J. Am. Ceram. Soc. 73 (5) (1990) 1117–1135.

[5] V.M.B. Moloney, D. Parris, M.J. Edirisinghe, Rheology of zirconia suspensions in a nonpolar organic medium, J. Am. Ceram. Soc. 78 (12) (1995) 3225–3232.

[6] G. Wang, P.S. Nicholson, Influence of acidity on the stability and rheological properties of ionically stabilized alumina suspensions in ethanol, J. Am. Ceram. Soc. 84 (9) (2001) 1977–1980.

[7] A.J. Sánchez-Herencia, A.J. Millán, M.I. Nieto, R. Moreno, Aqueous colloidal processing of nickel powder, Acta Mater. 49 (2001) 645–651.

[8] F.F. Lange, Powder processing science and technology for increased reliability, J. Am. Ceram. Soc. 72 (1) (1989) 3–15.

[9] J.A. Lewis, Colloidal processing of ceramics, J. Am. Ceram. Soc. 83 (2000) 2341–2359.

[10] L. Bergström, Surface and Colloid Chemistry in Advanced Ceramics Processing, Marcel Dekker, Inc, New York, 1994.

[11] D.J. Shanefield, Organic Additives and Ceramic Processing, Kluwer Academic Publishers, Boston, 1996.

[12] J.S. Reed, Principles of Ceramics Processing, Wiley and Sons, Inc, New York, 1995.

[13] W.J. Tseng, K.-H. Teng, The effect of surfactant adsorption on sedimentation behaviors of Al_2O_3-toluene suspensions, Mater. Sci. Eng. A 318 (2001) 102–110.

[14] J.J. Guo, J.A. Lewis, Effects of ammonium chloride on the rheological properties and sedimentation behavior of aqueous silica suspensions, J. Am. Ceram. Soc. 83 (2) (2000) 266–272.

[15] C. Allain, M. Cloitre, M. Wafra, Aggregation and sedimentation in colloidal suspensions, Phys. Rev. Lett. 74 (8) (1995) 1478–1481.

[16] W.J. Tseng, S.-Y. Li, Rheology of colloidal $BaTiO_3$ suspension with ammonium polyacrylate as a dispersant, Mater. Sci. Eng. A 333 (1-2) (2002) 314–319.

[17] W.J. Tseng, C.H. Wu, Aggregation, rheology and electrophoretic packing structure of aqueous Al_2O_3 nanoparticle suspensions, Acta Mater. 50 (15) (2002) 3757–3766.

[18] N. Casson, in: C.C. Mills (Ed.), Rheology of Disperse Systems, Pergamon, New York, 1959, pp. 84.